Burago N.G., Zhuravlev A.B., Nikitin I.S. Models of multiaxial fatigue and life time estimation of structures \\ Mechanics of Solids, 2011. N. 6. P. 22-33.

Models of Multiaxial Fatigue Fracture and Service Life Estimation of Structural Elements

N. G. Bourago[1], A. B. Zhuravlev[2], and I. S. Nikitin[3]

[1] *Ishlinsky Institute for Problems in Mechanics. Russian Academy of Sciences. pr-t Vernadskogo 101, str. I, Moscow., 119526 Russia*
[2]*Joint Institute for High Temperatures. Russian Academy of Sciences. Izhorskaya13-2. Moscow , 125412 Russia*
[3]*Moscow State Aviation Technological University, Orshanskaya 3, Moscow, 121552 Russia*

Abstract—We study criteria and models of multiaxial fracture under the conditions of low-cycle fatigue (L.CF). The model parameters are determined by using the data of uniaxial fatigue tests for different coefficients of the cycle asymmetry. A procedure for calculating the stress state of the compressor disk in a gas turbine engine (GTE) in the flight cycle of loading is outlined. The calculated stress state and models of multiaxial fatigue fracture are used to estimate the service life of the compressor disk. The results are compared with the observational data collected during the operation.

Keywords: *multiaxial fatigue fracture model, service life estimation, stress concentration, centrifugal load, aerodynamic load.*

1. INTRODUCTION

In the present paper, we outline the basic models of multiaxial fatigue fracture under the conditions of low-cycle fatigue (LCF) and give an example of using them to estimate the service life of elements of a specific engineering structure.

At present, there are several basic types of criteria and models of fatigue fracture which permit estimating the number of loading cycles that a material sample or a structural element can endure before failure; the criteria are based on evaluating the stress state, strain state, or accumulated fatigue. The determination of the parameters of the models under study is a fairly difficult experimental problem; it is carried out, as a rule, by using the results of uniaxial fatigue tests in tension, torsion, or bending with different coefficients of the cycle asymmetry.

Here we do not consider approaches related to studying the kinetics of fatigue crack growth versus the number of loading cycles and the stress state type.

As an example, we solve the problem of fatigue fracture of the compressor disk in a gas turbine engine (GTE, series D30) in flight loading cycles. We outline a computational procedure for determining the stress-strain state (SSS) of the contact system of the compressor disk and blades. The calculated SSS and chosen criteria and models of different typos are used to estimate the compressor disk service life under conditions that simulate the operating conditions.

2. STATEMENT OF THE PROBLEM

2.1. Estimation Models Bused on the Stress-Strain State

The determination of the parameters of multiaxial fatigue fracture is based experimental curves of uniaxial cyclic tests for different values of the cycle asymmetry parameter $R = \sigma_{\min} / \sigma_{\max}$ where $\sigma_{\max}$ and $\sigma_{\min}$ are the maximum and minimum stresses in the cycle. The uniaxial fatigue strength tests are usually described using the following notation: $\sigma_a = (\sigma_{\max} - \sigma_{\min})/2$ is the stress

amplitude in a cycle and $\Delta\sigma = \sigma_{\max} - \sigma_{\min}$ is the stress range in a uniaxial loading cycle.

One uses two types of representation of uniaxial fatigue tests in the form of an experimental dataset (and/or the corresponding approximating curves) of $\sigma_a(N)$ and $\sigma_{\max}(N)$ that show, for different values of the asymmetry parameter R the limit value of cycles N before fracture for fixed values of the stress amplitude $\sigma_a(N)$ (first type) or the maximum stress $\sigma_{\max}(N)$ (second type).

The experimental data of uniaxial tests are described by Weller curves, which can analytically be represented by the Baskin relation [1-3]

$$\sigma = \sigma_u + \sigma_c N^{\beta} \tag{2.1}$$

where σ_u is the fatigue limit, σ_c is the fatigue strength coefficient, β is the fatigue strength exponent, and N is the number of cycles before fracture. Typical results for titanium alloy [4, 5] are shown in Fig. 1.

The problem of studying fatigue fracture implies that the spatial distribution of a function of the number of cycles N before fracture must be determined from equations of the form (2.1) generalized to the case of multiaxial stress state and containing the calculated stresses in the structure under study.

If the dependence $\sigma_a(N)$ is represented in the form $\sigma_a = \sigma_u + \sigma_c N^{\beta}$ for $R = -1$ and $\sigma_a = \sigma_{u0} + \sigma_{c0} N^{\beta}$ for $R = 0$, then the corresponding curve $\sigma_{\max}(N)$ is expressed as

$$\sigma_{\max} = \sigma_u + \sigma_c N^{\beta} \text{ for } R = -1 \tag{2.2}$$

$$\sigma_{\max} = 2\sigma_{u0} + 2\sigma_{c0} N^{\beta} \text{ for } R = 0 \tag{2.3}$$

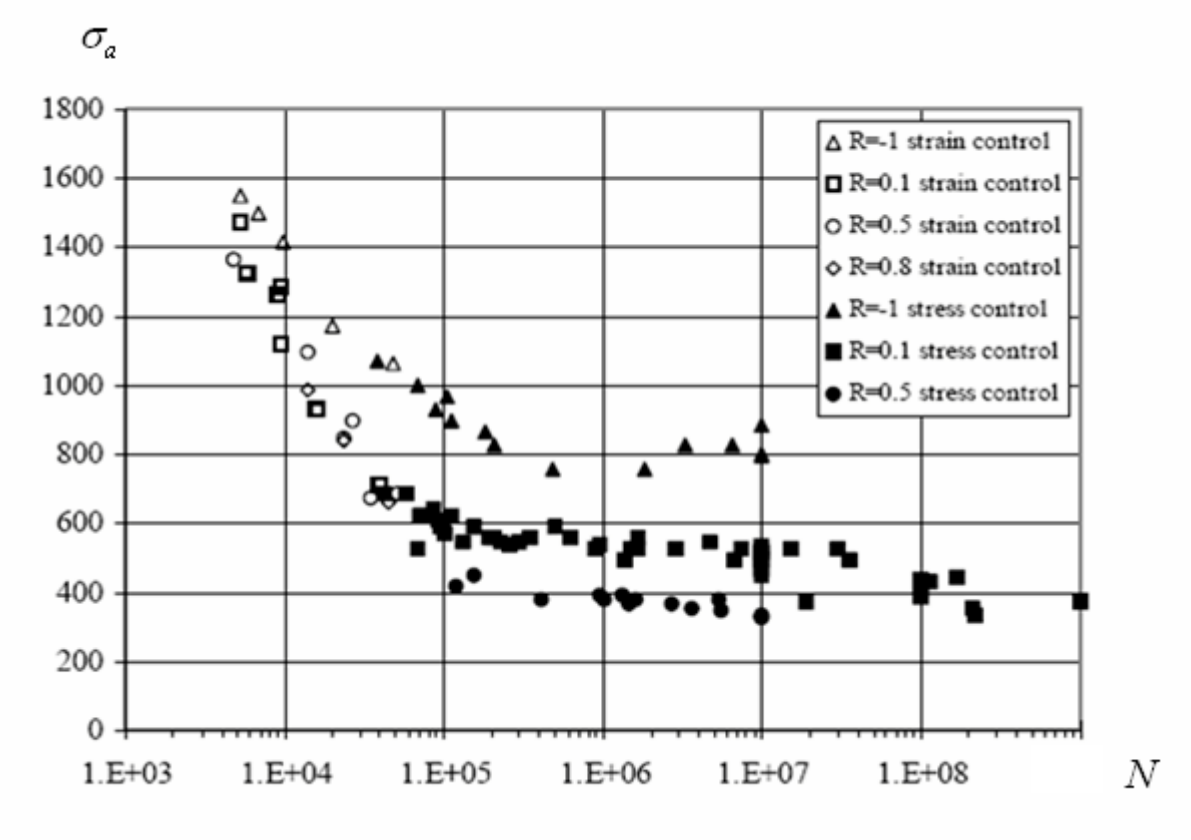

Fig.1

The ratio of the fatigue limits according to the curves $\sigma_{\max}(N)$ for $R = -1$ and $R = 0$ is equal

to $k_{-1} = \sigma_u /(2\sigma_{u0})$, where σ_u and σ_{u0} are the fatigue limits according to the curves $\sigma_a(N)$ for R = –1 and R = 0, respectively.

Let us consider the basic ways of generalizing the results of uniaxial tests to the case of multiaxial stress state.

2.1.1. Sines model. According to [6], the uniaxial fatigue curve (2.1) can be generalized to the case of multiaxial stress state as

$$\Delta\tau/2 + \alpha_s\sigma_{\text{mean}} = S_0 + AN^{\beta}, \quad \sigma_{\text{mean}} = (\sigma_1+\sigma_2+\sigma_3)_{\text{mean}}, \tag{2.4}$$

$$\Delta\tau = \sqrt{(\Delta\sigma_1-\Delta\sigma_2)^2+(\Delta\sigma_1-\Delta\sigma_3)^2+(\Delta\sigma_2-\Delta\sigma_3)^2}/3$$

where σ_{mean} is the mean sum of principal stresses over a loading cycle, $\Delta\tau$ is the change in the octahedral tangent stress per cycle, $\Delta\tau/2$ is the octahedral tangent stress amplitude, and α_s, S_0, A and β are parameters to he determined from experimental data.

To determine the model parameters from uniaxial fatigue curves, let us rewrite the equation of the uniaxial curve $\sigma_{\max}(N)$ for R = –1 and R = 0.

For R = – 1, we have $\Delta\tau/2 = \sqrt{(2\sigma_{\max})^2+(2\sigma_{\max})^2}/6 = \sqrt{2}\sigma_{\max}/3$ and $\alpha_s\sigma_{\text{mean}} = 0$, which implies that $\sqrt{2}\sigma_{\max}/3 = S_0 + AN^{\beta}$. Comparing with the uniaxial representation (2.2), we can obtain the relations $S_0 = \sqrt{2}\sigma_u/3$ and $A = \sqrt{2}\sigma_c/3$.

For R = 0, we have $\Delta\tau/2 = \sqrt{(\sigma_{\max})^2+(\sigma_{\max})^2}/6 = \sqrt{2}\sigma_{\max}/6$ and $\alpha_s\sigma_{\text{mean}} = \alpha_s\sigma_{\max}/2$. As a result, we obtain $(\sqrt{2}/6+\alpha_s/2)\sigma_{\max} = S_0 + AN^{\beta}$. Formula (2.3) implies the relation $S_0 = 2\sigma_{u0}(\sqrt{2}/6+\alpha_s/2)$. Equating the values of S_0, we find the parameter $\alpha_s = \sqrt{2}(2k_{-1}-1)/3$.

Here we note the following fact. The representation of the uniaxial fatigue curves by relation (2.1) is valid starting from the level of $N \sim 1000$; before these values, $\sigma(N)$ changes insignificantly and equals the tensile strength σ_B in order of magnitude [1, p. 378] as shown in Fig. 2. Therefore, to estimate the parameter A, we use the approximate relation $\sqrt{2}\sigma_B/3 = S_0 + 10^{3\beta}A$.

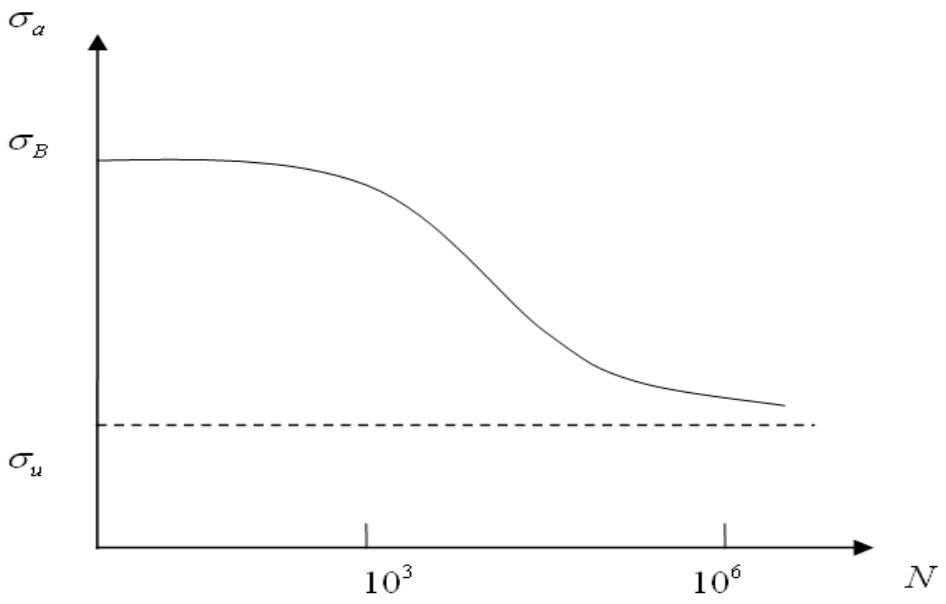

Fig.2

Let us write out the final expressions for the multiaxial model parameters in terms of the uniaxial fatigue curves for $R = -1$ and $R = 0$:

$$S_0 = \sqrt{2}\sigma_u / 3, \quad A = 10^{-3\beta}\sqrt{2}(\sigma_B - \sigma_u)/3, \quad \alpha_s = \sqrt{2}(2k_{-1} - 1)/3, \quad k_{-1} = \sigma_u / (2\sigma_{u0}) \tag{2.5}$$

2.1.2. Crossland model. According to [7], the uniaxial fatigue curve can be generalized to the case of multiaxial stress state as

$$\Delta\tau / 2 + \alpha_c(\overline{\sigma}_{\max} - \Delta\tau / 2) = S_0 + AN^{\beta}, \quad \overline{\sigma}_{\max} = (\sigma_1 + \sigma_2 + \sigma_3)_{\max} \tag{2.6}$$

where $\overline{\sigma}_{\max}$ is the maximum sum of principal stresses in a loading cycle; the parameters α_c, S_0, A and β are to be determined.

To determine the model parameters from uniaxial fatigue curves, we rewrite its equation for the uniaxial curve $\sigma_{\max}(N)$ for $R = -1$ and $R = 0$.

For $R = -1$, we have $\Delta\tau / 2 = \sqrt{(2\sigma_{\max})^2 + (2\sigma_{\max})^2}\,/6 = \sqrt{2}\sigma_{\max}/3$ and $\alpha_c\overline{\sigma}_{\max} = \alpha_c\sigma_{\max}$. Therefore, $\left(\sqrt{2}/3 + (1 - \sqrt{2}/3)\alpha_c\right)\sigma_{\max} = S_0 + AN^{\beta}$.

Comparing with the uniaxial representation $\sigma_{\max} = \sigma_u + \sigma_c N^b$ we obtain $S_0 = \left(\sqrt{2}/3 + (1 - \sqrt{2}/3)\alpha_c\right)\sigma_u$, $A = \left(\sqrt{2}/3 + (1 - \sqrt{2}/3)\alpha_c\right)\sigma_c$.

For $R = 0$, we obtain the expressions $\Delta\tau / 2 = \sqrt{(\sigma_{\max})^2 + (\sigma_{\max})^2}\,/6 = \sqrt{2}\sigma_{\max}/6$ and $\alpha_c\overline{\sigma}_{\max} = \alpha_c\sigma_{\max}$. As a result, we have $\left(\sqrt{2}/6 + (1 - \sqrt{2}/6)\alpha_c\right)\sigma_{\max} = S_0 + AN^{\beta}$. Comparing with the uniaxial representation $\sigma_{\max} = 2\sigma_{u0} + 2\sigma_{c0}N^{\beta}$, we obtain $S_0 = 2\sigma_{u0}\left(\sqrt{2}/6 + (1 - \sqrt{2}/6)\alpha_c\right)$. Equating the values of S_0, we find $\alpha_c = (k_{-1}\sqrt{2}/3 - \sqrt{2}/6)\Big/\left[(1 - \sqrt{2}/6) - k_{-1}(1 - \sqrt{2}/3)\right]$.

Repeating the argument used to determine the parameters of the Sines model, we determine a refined value of A. The final expressions relating the parameters of the multiaxial model to those of the uniaxial fatigue curves for $R = -1$ and $R = 0$ have the form

$$S_0 = \sigma_u\left[\sqrt{2}/3 + (1 - \sqrt{2}/3)\alpha_c\right], \quad A = 10^{-3b}\left[\sqrt{2}/3 + (1 - \sqrt{2}/3)\alpha_c\right](\sigma_B - \sigma_u) \tag{2.7}$$

$$\alpha_c = (k_{-1}\sqrt{2}/3 - \sqrt{2}/6)\Big/\left[(1 - \sqrt{2}/6) - k_{-1}(1 - \sqrt{2}/3)\right]$$

The parameters σ_u, σ_{u0}, σ_c and the exponent β for different materials are determined from the data of uniaxial fatigue tests for different coefficients of the cycle asymmetry.

Here are approximate values of the parameters for titanium alloy Ti-6Al-4V [4, 5] for a specific computational example that will be considered below: the limit strength is $\sigma_B = 1100$ MPa, the fatigue limits according to the curves $\sigma_a(N)$ for $R = -1$ and $R = 0$ are equal $\sigma_u = 450$ MPa and $\sigma_{u0} = 350$ MPa, respectively, the exponent in the power-law dependence on the number of cycles is $\beta = -0.45$, Young's modulus is $E = 116$ GPa, the shear modulus is $G = 44$ GPa, and Poisson's ratio is $\nu = 0.32$.

2.2. Estimation Models Based on the Strain State

The classical Coffin—Manson relation [1] describing the uniaxial fatigue fracture on the basis of the strain change per loading cycle has the form

$$\frac{\Delta\varepsilon}{2} = \frac{\sigma_c}{E}(2N)^b + \varepsilon_c(2N)^c$$

where σ_c is the (axial) fatigue strength coefficient, ε_c is the (axial) fatigue plasticity coefficient, and *b* and *c* are the fatigue strength and fatigue plasticity exponents.

Briefly outlined below are models generalizing the Coffin-Manson relation to the case of multiaxial fatigue fracture. The fatigue fracture mechanisms underlying each of the models listed below are illustrated by figs. 3 a, b, c [8].

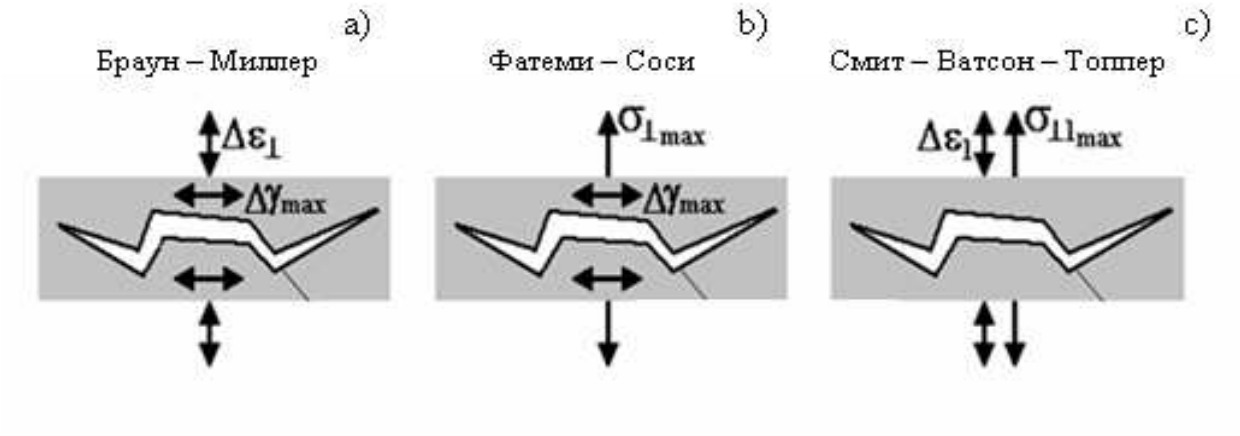

Fig.3

2.2.1. Brown-Miller model. The model was proposed in [9]; the corresponding fatigue fracture mechanism is illustrated in fig. 3 a. This model takes into account the influence of the normal strains to the plane of maximum shear strains:

$$\frac{\Delta\gamma_{\max}}{2} + \alpha_{bm}\Delta\varepsilon_{\perp} = \beta_1\frac{\sigma_c - 2\sigma_{\perp\text{mean}}}{E}(2N)^b + \beta_2\varepsilon_c(2N)^c \qquad (2.8)$$

where $\gamma_{ij} = 2\varepsilon_{ij}$, ε_{ij} are the strain tensor components, $\Delta\gamma_{\max}/2$ is the range of the maximum shear strains attained on a plane, $\Delta\varepsilon_{\perp}$ is the range of the normal strains on this plane, and $\sigma_{\perp\text{mean}}$ is the cycle-average normal stress on this plane. Approximate values of the coefficients are given in [8]: $\alpha_{bm} = 0.3$, $\beta_1 = (1+\nu)+(1-\nu)\alpha_{bm}$, $\beta_2 = 1.5 + 0.5\alpha_{bm}$.

2.2.2. Fatemi-Socie model. The model was proposed and developed in [10—13]; the fatigue fracture mechanism is illustrated in Fig. 3 b. This model takes into account the influence of the normal stresses to the plane of maximum shear strains:

$$\frac{\Delta\gamma_{\max}}{2}\left(1 + k\frac{\sigma_{\perp\max}}{\sigma_y}\right) = \frac{\tau_c}{G}(2N)^{b_0} + \gamma_c(2N)^{c_0} \qquad (2.9)$$

Here $\sigma_{\perp\max}$ is the cycle-maximum normal stress on the plane where $\gamma_{\max}$ is attained, σ_y is the material yield strength, τ_c is the fatigue (shear) strength coefficient, γ_c is the fatigue (shear) plasticity coefficient, and b_0 and c_0 are the fatigue strength and fatigue plasticity exponents. The coefficient *k* is approximately equal to *k* = 0.5 [13].

2.2.3. Smith-Watson-Topper model. The model was proposed in [14]; the fatigue fracture mechanism is illustrated in Fig. 3c. This model takes into account the influence of the normal stress to the plane of maximum tensile strains:

$$\frac{\Delta\varepsilon_1}{2}\sigma_{\perp 1\max} = \frac{\sigma_c^{\,2}}{E}(2N)^{2b} + \sigma_c\varepsilon_c(2N)^{b+c} \tag{2.10}$$

where $\Delta\varepsilon_1$ is the change in the maximum principal strain per cycle and $\sigma_{\perp 1\max}$ is the maximum normal stress on the plane of maximum tensile strains.

The fatigue parameters of titanium alloys for this class of models were chosen as follows.

In [15], the parameter estimate $\sigma_c = 1.67\sigma_B$ is given, and in [16], this parameter is estimated as $\sigma_c = \sigma_B + 345$ MPa. In [15-17], the (axial) fatigue parameters are estimated as follows: $\varepsilon_c = 0.35$, $b = -0.095$, $c = -0.69$. For shear fatigue parameters, the following relations are given in [8]: $\tau_c = \sigma_c/\sqrt{3}$, $\gamma_c = \varepsilon_c/\sqrt{3}$, $b = b_0$, $c = c_0$.

Finally, it was assumed in the calculations that $\sigma_c = 1445$ MPa, $\varepsilon_c = 0.35$, $b = -0.095$, $c = -0.69$, $\tau_c = 835$ MPa, $\gamma_c = 0.20$, $b_0 = -0.095$, $c_0 = -0.69$, and $\sigma_y = 910$ MPa.

We note that similar values of parameters are given in [13]: $\sigma_c = 1180$ MPa, $\varepsilon_c = 0.278$, $b = -0.025$, $c = -0.665$, $\tau_c = 881$ MPa, $\gamma_c = 0.18$, $b_0 = -0.082$, and $\sigma_y = 910$ MPa.

2.3. Models of Fatigue Fracture with Damage

2.3.1. Lemaitre-Chaboche model. In [18—20], the following differential equation for the damage D accumulated under multiaxial cyclic loading was suggested:

$$\frac{dD}{dN} = \left[1-(1-D)^{\beta+1}\right]^{\alpha}\left[\frac{A_{IIa}}{M_0(1-3b_2\overline{\sigma})(1-D)}\right]^{\beta}, \quad \alpha = 1 - a\left\langle\frac{(A_{IIa}-A^*)}{(\sigma_u-\sigma_{VM})}\right\rangle, \quad 0 \le D \le 1$$

Integrating yields

$$N = \frac{1}{(1+\beta)a_M}\left[\frac{(1-3b_2\overline{\sigma})}{A_{IIa}}\right]^{\beta}\left\langle\frac{(\sigma_u-\sigma_{VM})}{(A_{IIa}-A^*)}\right\rangle \tag{2.11}$$

where the notation from [20] is preserved:

$$A_{IIa} = 0.5\sqrt{1.5\left(S_{ij,\max}-S_{ij,\min}\right)\left(S_{ij,\max}-S_{ij,\min}\right)}, \quad \sigma_{VM} = \sqrt{0.5S_{ij,\max}S_{ij,\max}}$$

$$\overline{\sigma} = (\sigma_1+\sigma_2+\sigma_3)_{\text{mean}}/3, \quad A^* = \sigma_{10}\left(1-3b_1\overline{\sigma}\right), \quad a_M = a/M_0^{\beta}$$

where $S_{ij,\max}$ and $S_{ij,\min}$ are the maximum and minimum values of the stress deviator in the loading cycle; the angle brackets are defined as: $\langle X\rangle = 0$ for $X < 0$ and $\langle X\rangle = X$ for $X \ge 0$. The model parameters for a titanium alloy are given in [20]: $\beta = 7.689$, $b_1 = 0.0012$, $b_2 = 0.00085$ 1/MPa, $a_M = 4.1\cdot 10^{-28}$, $\sigma_{10} = 395$ MPa, and $\sigma_u = 1085$ MPa.

2.3.2. LU model (Liege University). This model was proposed and validated in [5]. In this case, the integrated differential equation for the damage gives

$$N = \frac{\gamma+1}{C}\left\langle\frac{\sigma_u-\theta\cdot\sigma_{VM}}{A_{IIa}-A^*}\right\rangle f_{\text{cr}}^{-(\gamma+1)} \tag{2.12}$$

where the notation of [5] is preserved:

$$f_{\text{cr}} = \frac{1}{b}\left(A_{IIa} + a\sigma_H - b\right), \quad f_{\text{cr}} > 0 \quad , \quad A^* = \sigma_{-1}\left(1 - 3s\sigma_H\right) \quad , \qquad \sigma_H = (\sigma_1 + \sigma_2 + \sigma_3)_{\max} / 3$$

The model parameters [5] have the following values: a=0.467, b=220 MPa, γ=0.572, $C = 7.12 \cdot 10^{-5}$, θ=0.75, s=0.00105 1/MPa, σ_{-1}=350 MPa, σ_u=1199 MPa.

3. EXAMPLE OF MUFTIAXIAL STRESS STATE CALCULATION AND SERVICE LIFE ESTIMATION FOR STRUCTURAL ELEMENTS

3.1. Computational Model of the Compressor Disk

As an example, we consider the problem of fatigue fracture of the compressor disk of a gas turbine engine in flight loading cycles under the conditions of low-cycle fatigue.

Below we outline the computational procedure for determining the SSS of a contact system consisting of the compressor disk and blades in the flight mode and present the computational results. A survey of papers on this topic can be found in [21]. On the basis of chosen criteria and different models, the SSS computation results are used to estimate the service life of the compressor disk under the conditions simulating the operational conditions.

It is assumed that the cycle of multiaxial loading of the disk-blade system is the flight loading cycle (FLC), in which the maximum loads at the aircraft cruising speed and the corresponding angular velocities of rotation of the compressor disk are attained. The problem is to determine the disk service life N (the number of FLCs before fracture) from relations (2.4), (2.6), and (2.8)-(2.12).

To this end, it is necessary to calculate the SSS of the disk-blade system under the combined action of the external loads, represented by the centrifugal forces, the distributed aerodynamic pressures on the blades, and the forces of nonlinear contact interaction between the disk, blades, and any other additional structural elements that are taken into account; these elements will be discussed below.

At present, there are modern software packages that can be used to solve coupled three-dimensional problems of gas dynamics and solid mechanics. However, the personal computers are insufficiently fast to obtain solutions to such problems efficiently. Therefore, in the present paper, the three-dimensional stress-strain stale of the contact system of the compressor disk and blades (Figs. 4 and 5) is analyzed numerically using a finite-element software package [22], and the distributed aerodynamic loads are determined approximately by analytical methods based on the use of classical solutions to the problem of flow about a grid of plates at an arbitrary angle of attack; the solutions are obtained by the complex analysis methods on the basis of the isolated profile hypothesis [21, 23, 24] with the blade strain state taken into account.

A blade is assumed to be a thin rectangular plate of width $2a$ with a varying twist $\gamma(r)$. We use the following notation: v_∞, p_∞ and ρ are the velocity, pressure, and gas density at infinity, x is the coordinate of points of the plate, $|x| \le a$, and r is the radial coordinate of the plate. The local angle of attack of the plate is equal to $\alpha(r) = \gamma(r) - \operatorname{arctg}(v_\infty/(\omega r))$. The local step of the blade grid is equal to $d = 2\pi r / N_1$, where N_1 is the number of blades on the disk.

The formula for the pressure drop on the surface of a blade was obtained in [21]:

$$\Delta p(r, x) = \rho\left(v_\infty^2 + \omega^2 r^2\right)\exp\left(-aN_1/2r\right)\sin 2\alpha(r)\sqrt{\operatorname{sh}\frac{N_1(a-x)}{2r}\Big/\operatorname{sh}\frac{N_1(a+x)}{2r}} \qquad (3.1)$$

The gas compressibility was taken into account by introducing the Prandtl-Glauert multiplier $1/\sqrt{1-M^2}$, where M is the Mach number of the incident flow, $M = w/c = \sqrt{v_\infty^2 + \omega^2 r^2}/c$, c is the

sound speed, and $\Delta p^c(r,x) = \Delta p(r,x)/\sqrt{1-M^2}$.

The above formulas hold under the condition of subsonic flows, $\sqrt{v_\infty^2 + \omega^2 r^2} < c$, and were used to determine the distributed aerodynamic pressures on the blades in the stress-strain state calculations of the contact system.

The computational parameters were the following: the angular velocity of rotation ω = 314 rad/s (3,000 revolutions per minute), the dynamic velocity pressure at infinity $\rho v_\infty^2/2$ = 26,000 N/m^2, which corresponds to the flow speed 200 m/s with density 1.3 kg/m^3. The pressure on the blades was taken to be equal to the additional pressure given by (3.1). The total number of finite elements does not exceed 100,000, which is quite acceptable for computations on a personal computer. The material properties were as follows: E=116 GPa, ν =0.32, and ρ = 4370 kg/m^3 for the disk (titanium alloy), E = 69 GPa, ν = 0.33, and ρ = 2700 kg/m^3 for the blades (aluminum alloy), and E = 207 GPa, ν = 0.27, and ρ = 7860 kg/m^3 for the fixing pins (steel).

The computations were performed in two stages. At the first stage, on a coarse mesh, under the assumption of elastic behavior of the material, we calculated the deformation of the entire compressor disk together with the blades (Fig. 4) to determine the displacements at the boundary between a disk sector and a single blade (Fig. 5). At the second stage, a more accurate computation of the disk sector with the blade (Fig. 5) was performed on a refined mesh for given boundary displacements calculated at the first stage. The cylindrical pins fixing each blade to the disk and the bandage flanges were also taken into account. Their influence on the SSS is described in [25, 26].

The interaction of the aerodynamic loads with the strain state of the disk-blade system is taken into account in an iterative process of alternate refinement of the loads and the strain state [25, 26]. The computations showed that 3 or 4 iterations are required to attain an acceptable accuracy of the order of 1%. From the viewpoint of fatigue crack nucleation, the most dangerous areas are those near the "swallow tail" contact regions [21] between the disk and the blades. The computations showed that the best correspondence between the computational and experimentally observable stress concentration regions is attained when the possibility of detachment and slip of the disk and blade contact boundaries is taken into account. On the boundary of the fixing pin (Fig. 5), the conditions of complete adhesion were posed from technological considerations. Figure 6 shows the zone of concentration of maximum tensile stresses at the left (rounded) corner of the groove where the blade is inserted. One can see that the stress concentration increases from the front to the rear part of the groove, which coincides with the data on the location of fatigue crack nucleation regions in the rear part of the disk [2].

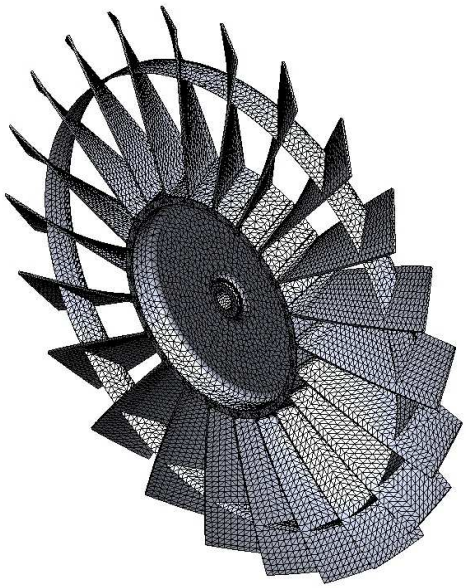

Fig.4

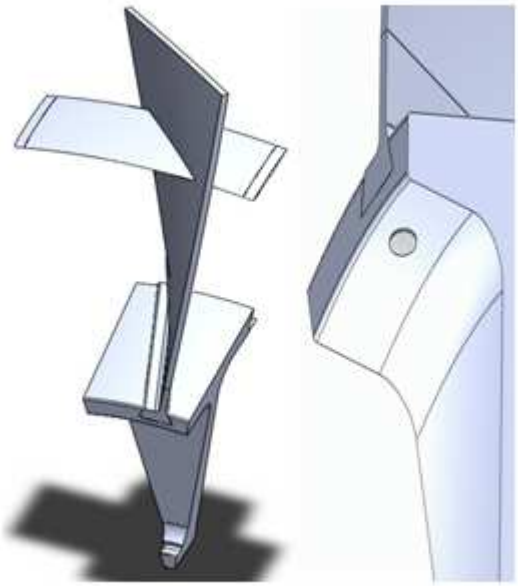

Fig.5

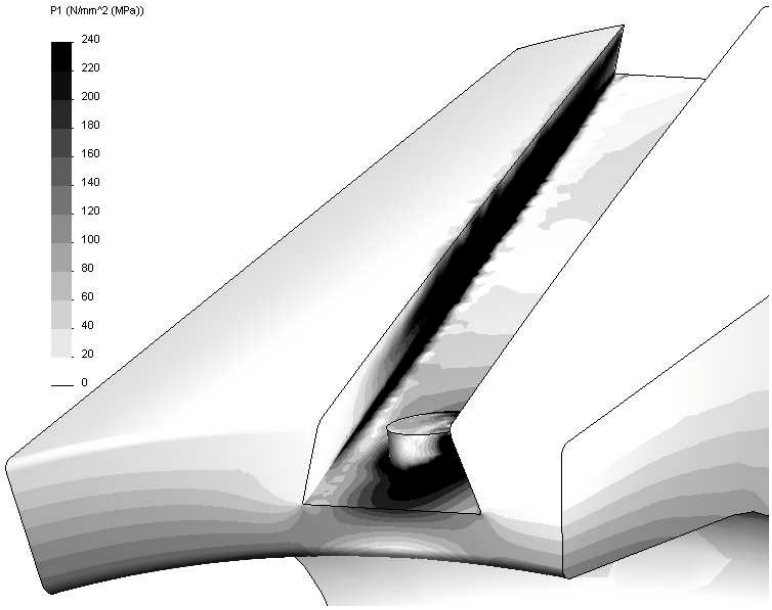

Fig.6

3.2. Service Life Estimation of Structural Elements

In Fig. 7, the computed values of the number *N* of flight cycles before fracture for the chosen criteria and models of multiaxial fatigue fracture are displayed near the left "swallow tail" disk-blade contact joint (in the regions of maximum stress concentration). In Fig. 8, the neighborhood of the left corner of the disk contact groove is shown by solid lines. In Fig. 7, the horizontal axis represents the dimensionless coordinates of the rounding of the groove's left corner; the vertical axis represents the dimensionless coordinate across the groove depth.

Burago N.G., Zhuravlev A.B., Nikitin I.S. Models of multiaxial fatigue and life time estimation of structures \\ Mechanics of Solids, 2011. N. 6. P. 22-33.

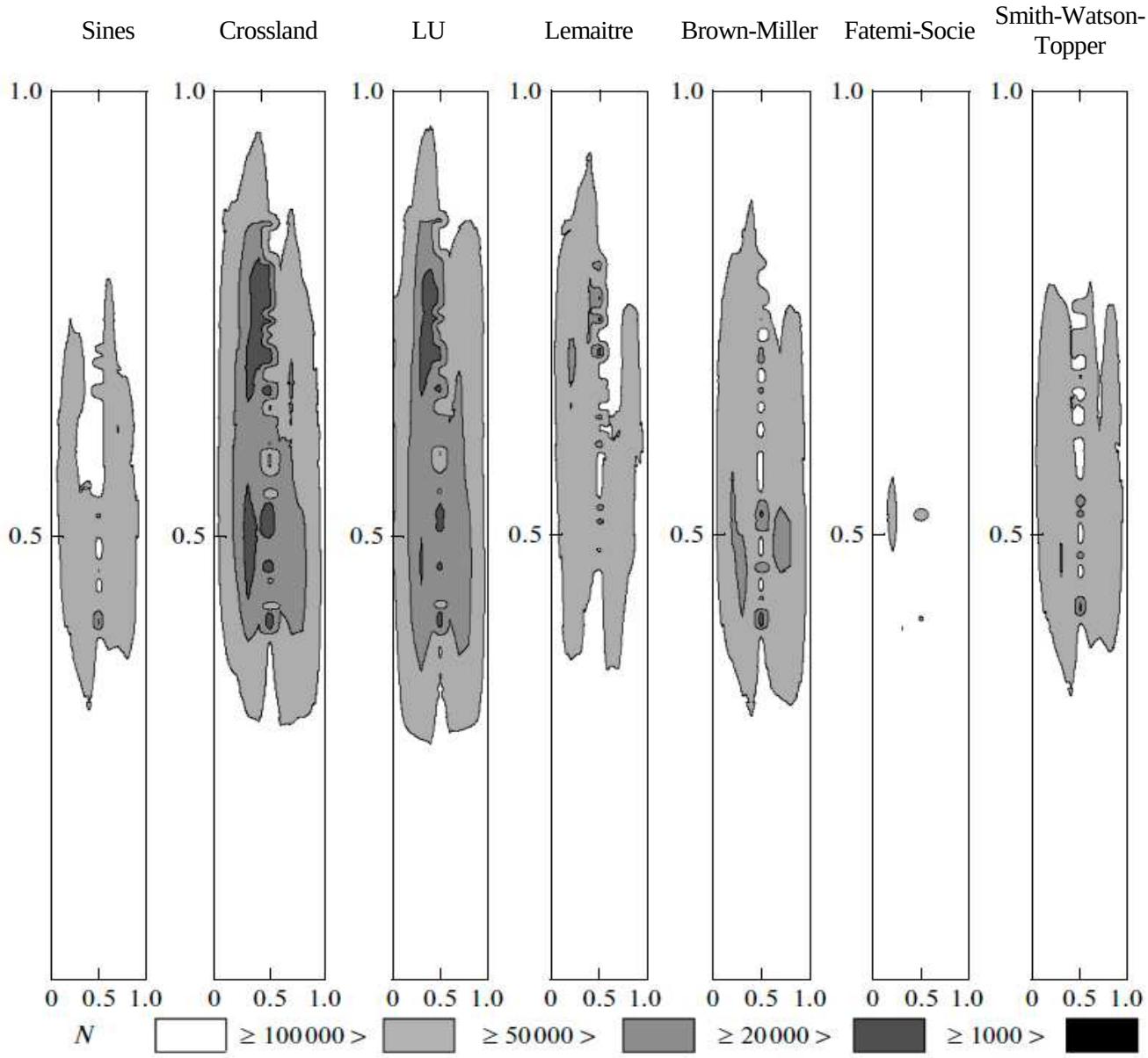

Fig.7

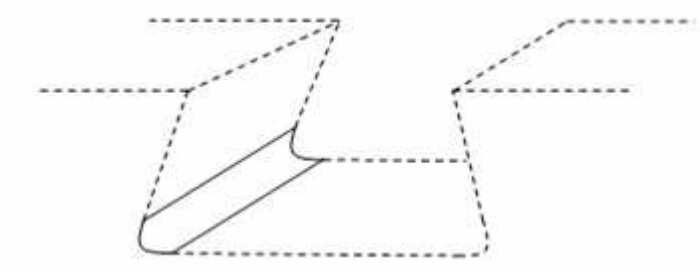

Fig.8

The above computational results for the stress-strain state and the estimation of the number of flight cycles before fracture N were compared with the results obtained in [2] by analyzing the observed laws of nucleation and growth of fatigue cracks during the operation of disks of the type in question.

The Sines, Lemaitre-Chaboche, Brown-Miller, and Smith-Watson-Topper criteria provided estimates of the service life of gas turbine engine disks around 20,000-50,000 cycles. The Crossland and LU criteria predicted the possibility of fatigue fracture after less than 20,000 flight cycles. On the whole, all these criteria give similar pictures of location of the fatigue fracture regions. The Fatemi-Socie criterion gives a service life prediction of about 100,000 cycles. The deviation of the Fatemi-Socie estimate from the results obtained based on the other criteria may testify that the shear mechanism of multiaxial fatigue fracture, which is reflected in this criterion, is not purely realized in flight loading cycles.

CONCLUSIONS

In the present paper, we have analyzed and identified parameters of multiaxial fracture criteria in the case of low-cycle fatigue (LCF) based on the consideration of the stress and strain states and accumulated damage.

We have presented an example of the utilizing different models for studying fatigue fracture of compressor disks of D30 gas turbine engines. For this purpose, we have developed a computational model of the compressor disk-blade contact system taking into account the aerodynamic and centrifugal loads, simulating the operational loads, and performed computations of the stress-strain state. Different criteria have been used to estimate the service life of the chosen structural elements, and these estimates correspond to the development of low-cycle fatigue fracture processes with the number of cycles before fracture of 10,000-100,000.

ACKNOWLEDGMENTS

The authors wish to thank A. A. Shanyavskii for valuable discussions of the results in the course of writing this paper.

The research was supported by the Federal Target Programme "Research and Pedagogical Cadre for Innovative Russia" for 2009-2013.

REFERENCES

1. J. A. Collins, *Failure o[Materials in Mechanical Design: Analysis. Prediction, Prevention* (Wiley, New York, 1981; Mir, Moscow, 1984).
2. A. Shanyavskii, *Modeling of Metal Fatigue fracture* (OOO "Monografiya". Ufa, 2007) [in Russian].
3. V. Bonnand, J.L. Chaboche, H. Cherouali, et al., “Investigation of Multiaxial Fatigue in the Prospect of Turbine Disc Applications: Part II – Fatigue Criteria Analysis and Formulation of a New Combined One,” in *Proc. 9-th Int. Conf. of Multiaxial Fatigue and Fracture (ICMFF9), Parma, Italy, 2010,* pp.691-698.
4. A.R. Kallmeyer, A. Krgo, and P. Kurath, “Evaluation of Multiaxial Fatigue Life Prediction Methodologies for Ti-6Al-4V,” Trans. ASME. J. Engng. Mater. Technol. **124** (2), 229-237 (2002).
5. A.K. Marmi, A.M. Habraken, and L. Duchene, “Multiaxial Fatigue Damage Modeling of Ti-6Al-4V Alloy,” in *Proc. 9 Int. Conf. of Multiaxial Fatigue and Fracture (ICMFF9), Parma,*

Italy, 2010, pp.559-567.

6. G. Sines, "Behavior of Metals under Complex Static and Alternating Stresses," in *Metal fatigue* (McGraw-Hill, London, 1958), pp. 145-169.
7. B. Crossland, "Effect of Large Hydrostatic Pressures on Torsional Fatigue Strength of an Alloy Steel," in *Proc. Int. Conf. on Fatigue of Metals* (London, 1956), pp.138-149.
8. M.A. Meggiolaro, A.C. Miranda, and J. de Castro, "Comparison among Fatigue Life Prediction Methods and Stress-Strain Models under Multiaxial Loading," in *Proc. 19th Int. Congr. of Mech. Eng. 2007, Brasilia, DF.*
9. M. Brown and K.J. Miller, "A Theory for Fatigue under Multiaxial Stress-Strain Conditions," Proc. Inst. Mech. Engineers **187** (65), 745-756 (1973).
10. A. Fatemi and D.F. Socie, "A Critical Plane Approach to Multiaxial Damage Including Out-of-Phase Loading," Fatigue Fract. Engng. Mater. Struct. **11** (3), 149-166 (1988).
11. D.F. Socie and G. B. Marquis, *Multiaxial fatigue* (Soc. Autom. Engineers, Pa., 2000)
12. N. Shamsaei, A. Fatemi, and D.F. Socie, "Multiaxial Fatigue Evaluation Using Discriminating Strain Paths," Int. J. Fatigue **33** (4), 597-609 (2011).
13. N. Shamsaei, M. Gladskyi, K. Panasovskyi K., et al., "Multiaxial Fatigue of Titanium Including Step Loading and Path Alternation and Sequence Affects," Int. J. Fatigue **32** (11), 1862-1874 (2010).
14. R.N. Smith, P. Watson, and T.H. Topper, "A Stress-Strain Parameter for the Fatigue of Metals," J. Mater. 5 (4), 767-778 (1970).
15. A. Baumel and T. Seeger, *Material Data for Cycling Loading, Supplement 1* (Elsevier, Amsterdam, 1990).
16. Y.-L. Lee, J. Pan, R.B. Hathaway, and M. Barkey, *Fatigue Testing and Analysis, Theory and Practice* (Elsevier, Oxford, 2005).
17. R. Bazan, M. Franulovic, I. Prebil, and N. Crnjaric-Zic, "Analysis of Strain-Life Fatigue Parameters and Behavior of Different Groups of Metallic Materials," Int. J. Fatigue **33** (3), 484-491 (2011).
18. J. Lemaitre and J.L. Chaboche, *Mechanics of Solid Materials* (Univ. Press. Cambridge, 1994).
19. J.L. Chaboche and P.M. Lesne, "Nonlinear Continuous Fatigue Model," Fatigue Fract. Engng. Mater. Struct. **11** (1) 1-17 (1988).
20. A.K. Marmi, A.M. Habraken, and L. Duchene, "Multiaxial Fatigue Damage Modeling at Macro Scale of Ti-6Al-4V Alloy," Int. J. Fatigue **31** (11), 2031-2040 (2009).
21. N.G. Burago, A.B. Zhuravlev, I.S. Nikitin, and V.S. Yushkov, *Study of Stress State of GTE Structural Elements*, Preprint No. 959 (IPMech RAN, Moscow, 2010) [in Russian].
22. A.A. Alyamovskii, A.A. Sobachkin, E.V. Odintsov, et al., SolidWorks: Computer Simulation in Engineering Practice (BKhv-Peterburg, St. Peterburg, 2005) [in Russian].
23. A.M. Mkhitaryan, *Aerodynamics* (Mashinostroenie, Moscow, 1976) [in Russian].
24. N.E. Kochin, I.A. Kibel, N.V. Roze, *Theoretical Hydrodynamics*, Part 1 (Fizmatgiz, Moscow, 1963; Interscience, New York, 1964).
25. N.G. Burago, A.B. Zhuravlev, I.S. Nikitin, *Aeroelastic Analysis of GTE Disk-Blade Contact System*, in *Proc. 22 Sci.-Tech. Conference o Aerodynamics* (TsAGI, Moscow, 2011) [in Russian].
26. N.G. Burago, A.B. Zhuravlev, I.S. Nikitin, "Analysis of Stress State of GTE Contact System 'Disk-Blade'," Vych. Mekh. Sploshn. Sred **4** (2), 5-16 (2011).